J Mater Sci (2007) 42:7408–7414
DOI 10.1007/s10853-007-1837-x

Effect of SiCp addition on age-hardening of aluminium composite and closed cell aluminium composite foam

V. Rajput · D. P. Mondal · S. Das · N. Ramakrishnan · A. K. Jha

Received: 10 February 2006 / Accepted: 22 January 2007 / Published online: 29 May 2007

Abstract The age hardening behavior of solid Al-alloy–SiCp composite and closed cell Al-alloy–SiCp composite cellular materials has been examined and compared. The peak aging period of these materials were also compared with that of the solid unreinforced alloy. The effect of SiCp content on the peak aging time has been examined. It was found that the composite aged faster than the alloy irrespective of SiCp content, wherein peak aging time was invariant to SiCp content. On the other hand, while the closed cell composite foam reached a peak aged condition faster than the alloy when SiCp content was less than 10 wt%, further increases in SiCp content delayed the age-hardening kinetics.

Introduction

Aluminium alloy particle reinforced composites have found a wide range of applications in automobile, aerospace, and other engineering applications [1–5]. These are due to the fact that these composite materials offer excellent combinations of physical, mechanical and tribological properties [6–9]. Further more, there is enough flexibility in design to tailor the materials for specific applications and for specific property requirements. Considerable work has been carried out on the synthesis and characterization of aluminium matrix composites. It is understood that the properties of the composite depends on several factors like distribution of particles, interface characteristics, and the shape, size and volume fraction of the reinforcements [10–12]. It is further understood that because of the significant differences in thermal expansion coefficient of the aluminium alloy matrix and SiCp, there exist significant thermal residual stresses around the particles within the matrix [13, 14]. This further leads to the following facts: (i) stress gradients or stress fields in the matrix, (ii) more dislocations in the matrix and (iii) elasto-plastic deformation of the matrix around the particles [10–12, 15–17]. All these factors influence the diffusion of elements within the matrix significantly and also alter the presence of the nucleation sites, which in other ways affect the precipitation behavior. Along these lines, a number of attempts have been made to examine the age-hardening kinetics of aluminum composites with respect to that of the alloy [16–24]. It is, in general, reported that the composite ages faster than the alloy. But the effect of SiC content on the aging kinetic of aluminium–SiCp composites has not been studied in detail.

In recent years, enormous attention are being paid on the development of lightweight cellular materials for energy and shock absorption, vibration control, sound absorption, heat exchanger applications etc., and a few demonstrative components have been produced especially for automobile applications [25–29]. The cellular structures contain closed and open cell pores, and have relative densities as low as 0.05 [29]. Because of these facts, the cellular structures have considerably higher surface area. The cells are stabilized with the addition of thickening agents like SiC particles or granular calcium during synthesis [30, 31]. The cell characteristics are reported to be a strong function of SiC content.

V. Rajput · D. P. Mondal (✉) · S. Das · N. Ramakrishnan
Advanced Materials and Processes Research Institute (CSIR), Bhopal 462026, India
e-mail: mondaldp@yahoo.com

A. K. Jha
Mechanical Engineering Department, Institute of Technology (BHU), Varanasi, India

In order to get variation in cell structures, SiC content in the cellular materials is varied [32]. Additionally, the plateau stress of cellular materials strongly depends on the matrix materials with which the cellular materials are made. Thus, the plateau stress of cellular materials could be a strong function of SiC content, relative density and the heat treatment schedule [32, 33]. But only limited studies have been conducted on the age-hardening of aluminum–SiC composite closed cell foam [33–36]. However, to the best of our knowledge, the effect of SiC content on the age hardening schedule and the kinetics of precipitation in Al–SiCp composite foam has not been studied. In addition, studies comparing the age-hardening behavior of solid composites and cellular composites are lacking.

In view of the above, the present paper aims at studying the effect of SiC content on age-hardening behavior of AA2014–SiCp composites and cellular composites produced using this matrix through a liquid metallurgy route. This paper examines the differences in age-hardening response of the cellular composite as compared to that of the fully dense composites.

Experimental

AA2014 Al–SiCp composites were synthesized using liquid metallurgy route following a stir-casting procedure. The process involved melting of alloy, incorporation of preheated SiC particles in the melt with the help of mechanical stirring, solidification of composite melt in a cylindrical cast iron permanent die having diameter of 30 mm and length of 200 mm. After casting the alloy, the same composite melt was used for preparation of AA2014–SiCp closed cell composite foam. The process of preparation of foam involved addition of preheated CaH_2 particles into the composite melt, allowing the melt to be in the crucible inside the furnace for foaming, ejection of the crucible containing foam from the furnace and rapid cooling with the compressed air. The size range of SiC particles ranged from 20 to 40 μm and its amount was varied from 5 to 20 wt% both in the fully dense composite and the composite foam. The size of CaH_2 varied in the range of 50 to 100 μm. For foaming 1.0 wt% CaH_2 was added to the composite melt.

Age-hardening schedule included homogenization at 495 °C for 8 h followed by oil quenching and then artificial aging for 2–12 h (at 2 h intervals) at a temperature of 175 °C followed by water quenching. Age-hardening behavior was studied through microhardness measurement on the samples as a function of aging time. For microhardness measurement, the samples were polished to mirror finish and then etched. Microhardness readings were taken in the matrix region in both the dense and cellular composite. In the case of cellular materials, microhardness readings were taken at the plateau region as it is the widest region of the cellular structures. Microhardness measurements were made in a LICA microhardness tester using a load of 10 gmf so that indentation size is limited to 10–12 μm, which are significantly less than the inter-particle spacing in the composite and the composite foam. For each specimen, at least 100 microhardness readings were taken and their average along with standard deviation was considered for the analysis.

For microstructural examinations, specimens of the fully dense aluminium composite and the alloy were prepared using standard metallographic technique. However, special care was taken for preparation of specimens for microstructural examinations of composite foams. Before grinding and polishing, thin samples were cut using a precision diamond cutter and then the pores of the samples were filled with cold mounting materials so that during grinding and polishing, the cell structures retained rigidity without any damage. After polishing, and etching with Nital, the samples were sputtered with gold prior to SEM examination. The cell size of the foam was determined using random intercept method as used for grain size measurement in metallographic technique. The cell wall thickness was determined from 100 individual measurements of cell walls from the magnified view of SEM micrograph.

Results and discussion

Materials and microstructures

The microstructure of dense AA2014–SiC composites exhibited uniform distribution of the particles (Fig. 1a) and sound bonding between SiC particle and the alloy matrix (Fig. 1b). The synthesized foam exhibited spatial distribution of cells (Fig. 2a). The cell size distribution of the synthesized foams made using 10 wt% SiC reinforced composite is shown in Fig. 2b. Similar type of distribution was noted in other foams as well. A higher magnification micrograph of foam sample is shown in Fig. 3a. It clearly indicates cell walls (marked by W), plateau regions (marked by P) and micro-pores in the plateau region and in the cell walls (marked by M). SiC particles were found to be present at the cell walls and at the plateau region (marked arrow). A few particles were also pushed towards the edge of the cell wall. It may be further noted that during foaming, a few cell walls ruptured (Fig. 3b). This might be attributed to the fact that foaming progresses by nucleation of micro-pores due to evolution of dissolved hydrogen gas or the hydrogen gas dissociated from added calcium hydride. Accumulation of gas leads to growth of the pores

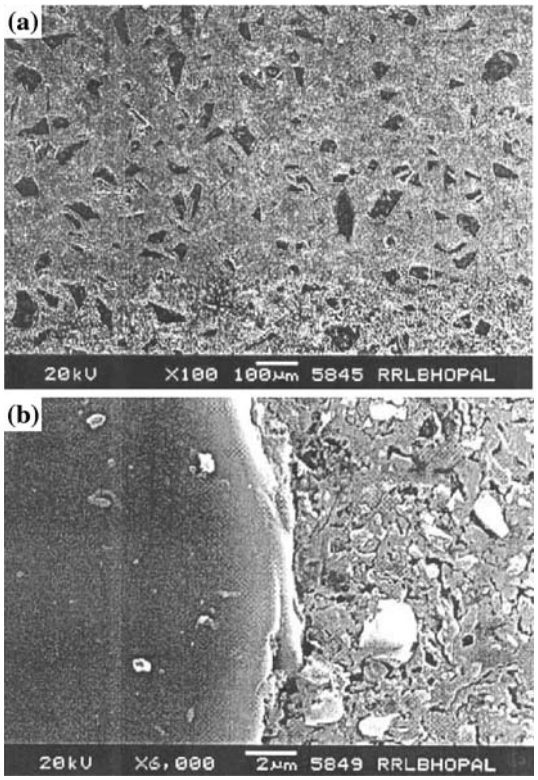

Fig. 1 (**a**) Secondary electron image showing the distribution of SiCp particles in the Aluminium alloy matrix. (**b**) Higher magnification view showing the interface between an SiCp particle and the Aluminium matrix

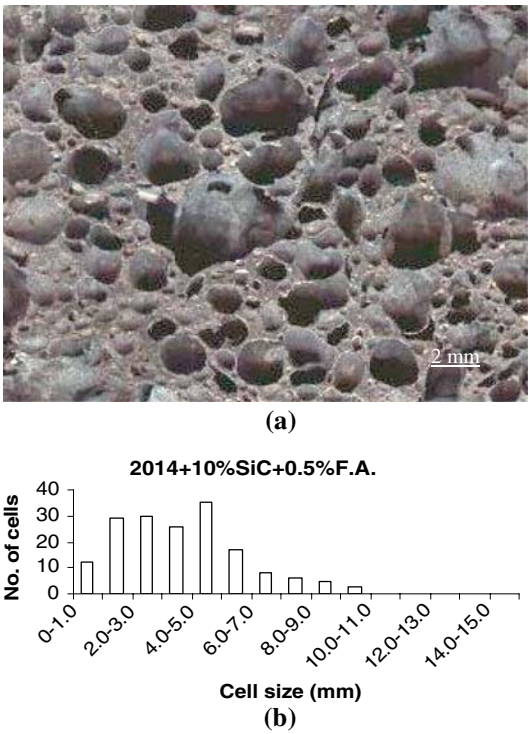

Fig. 2 (**a**) Typical optical image of closed cell aluminium foam structure showing the distribution of cell. (**b**) Bar graph showing the distribution pattern of cell size in the closed cell aluminium foam

or cells. In this process, micro-pores grow to a critical size and coalesce with other surrounding pores and thus the cells grow larger and larger in size. In this process a few cells are annihilated and cell wall become discontinuous. This also signifies that the synthesized foams are not absolutely closed pore foams. The bonding between SiC particles and the matrix is not as strong as that of the fully dense composite. This is due to accumulation of hydrogen gas at the SiC particle and matrix interface during the foaming process. It may clearly be noted that in the 20 wt% SiCp composite foam, the interface is very weak (Fig. 3c). The average cell size and cell wall thickness along with the associated standard deviation for the investigated foams, are reported in Table 1. It indicates that the cell wall thickness as well as cell size increases marginally with SiCp content [32]. This is primarily attributed to a lesser degree of drainage during foaming and because of higher viscosity at higher SiC content; the cells would grow to relatively larger sizes without collapsing or rupturing. Higher SiC content helps in retention of liquid melt for longer periods in the cell wall region and thus more liquid melt is accommodated at the cell wall. These in due course lead to an increase in cell wall thickness [30–32].

Age-hardening behavior in the fully dense composite

Average micro-hardness values as a function of aging time for the alloy and the composites are plotted in Fig. 4. In general, it may be noted that the microhardness values of the matrix increases with increases in SiCp content. This is primarily attributed to the existence of a higher dislocation density due to presence of a thermal residual stress field in the matrix [11, 24]. The stress field is generated due to differences in the thermal expansion coefficients of the SiCp and in the matrix [11, 24]. It is reported by a few investigators that this stress field in Al–SiCp composite could be of the order of yield stress or greater than the yield stress of the matrix [37]. It is further noted from this figure that average microhardness of the alloy and composite increases initially with aging time, attaining the peak value at a specific aging time (termed peak aging time). The peak aging time for the composite materials, irrespective of SiCp content, is noted to be 4 h, whereas the monolithic alloy reaches peak aged condition at 6 h aging time. This signifies that the composite ages faster than the alloy. This figure further demonstrates that the aging kinetics in the composite is invariant to SiCp content. The nature of age hardening curves is noted to be almost same. This signifies that the aging sequence in the alloy and composite remains unchanged. The nature of the curves, however,

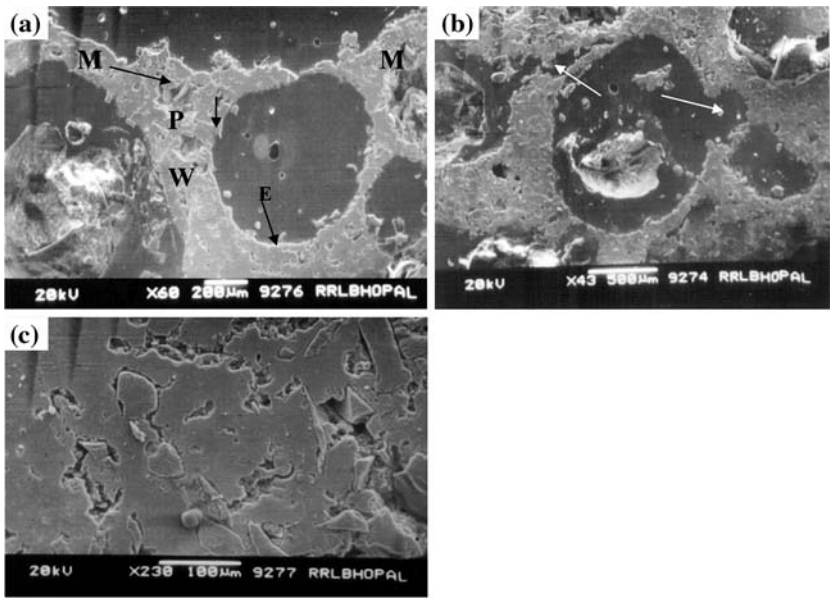

Fig. 3 Secondary electron images of: (**a**) the closed cell aluminium foam showing the cell shape, cell wall (W), plateau region (P) and cell edge (E); (**b**) a cell wall that ruptured during the growth of the cell and the incorporation/agglomeration of small cell into bigger one (arrow marked); and (**c**) the interface among SiCp particle and Aluminium matrix material at the plateau region of the closed cell aluminium foam

Table 1 Average cell size and cell wall thickness of closed cell composite foam

S. No.	Composition of foam	Density (gm/c.c.)	Average Pore Size (mm)	Cell wall thickness (µm)
1.	2014 + 5% SiCp + 0.5% Foaming agent	0.57	3.3 ± 0.2	205 ± 21
2.	2014 + 10% SiCp + 0.5% Foaming agent	0.59	3.9 ± 0.3	218 ± 25
3.	2014 + 20% SiCp + 0.5% Foaming agent	0.54	4.2 ± 0.2	235 ± 17

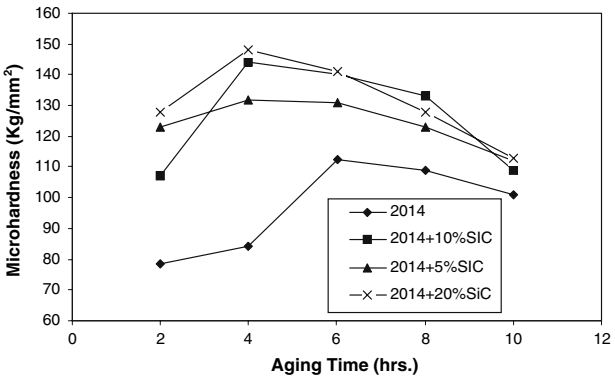

Fig. 4 Curves showing the microhardness of the 2014 aluminium alloy and different aluminium SiCp composites as a function of aging time

demonstrates that after peak aging the microhardness of composite drops at faster rate, indicating that over aging of the precipitates in composites is also faster than that of the alloy. Faster aging and coarsening in composite is primarily due to presence of excess dislocation density, thermal residual stress, which in other words increases potential sites for nucleation of precipitates and diffusivity of the elements. The aging or precipitation and precipitation coarsening process are nucleation and diffusion controlled processes. As a result, faster aging and faster over aging is noted in composite as compared to that of the alloy. The microstructure of peak aged and over aged matrix in the composite is shown in Fig. 5a and b, respectively, which demonstrates very fine precipitates in peak aged condition grow to considerably coarser size due to over aging.

In line with the above it may be realized that both the thermal stress as well as dislocation density increases with increase in SiCp content. However, because of higher SiCp content, the porosity level in the composite increases, which is indicated by their density (Table 2). Furthermore, the bonding between the alloy matrix and composite is of the mechanical type. Thus, the interface also acts as dislocation sink and stress releasing site. As a result, even with the increase in SiCp, overall dislocation density and thermal residual stress do not increase with increase in SiCp content. As a result, the age hardening kinetics remain invariant to SiCp content in the composite.

Age-hardening behavior of composite foam

Average microhardness values as a function of aging time for composite foam containing varying SiCp content is shown in Fig. 6. The microhardness values, in the case of

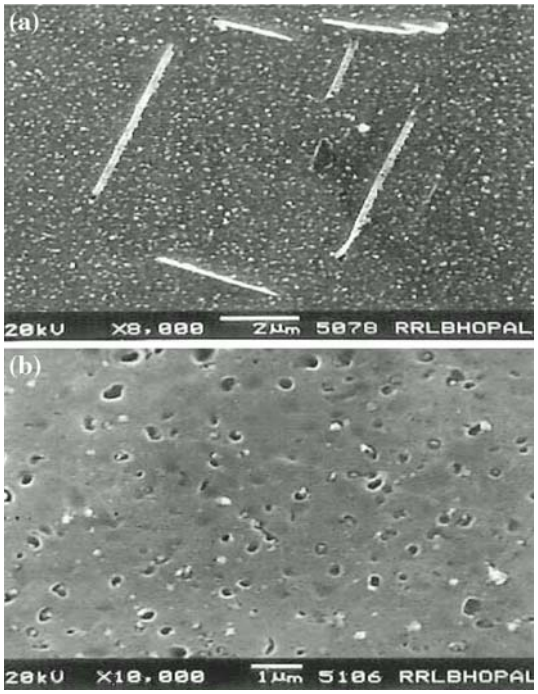

Fig. 5 Secondary electron images showing the matrix microstructure of the heat treated composite: (**a**) Peak aged and (**b**) Over aged

Table 2 Volume fraction of SiCp particles, density and porosity in alloy and composites

S. No.	Composition	Volume fraction Of SiCp (%)	Density (gm/c.c.)	Percentage Porosity (%)
1.	2014 Alloy	0.0	2.75	1.5
2.	2014 + 5% SiCp	5.	2.75	2.2
3.	2014 + 10% SiCp	11.2	2.71	3.3
4.	2014 + 20% SiCp	21.3	2.68	4.1

5 wt% and 10 wt% SiCp composite foam, increases with increased aging time and reaches the peak aged condition at 2 h and 4 h, respectively. It is further noted that after reaching peak aging, microhardness values decreased with aging time, indicating over aging. It is interesting to note, however, that microhardness values once again increases and exhibits a secondary peak at 8 h. This might be due to precipitation hardening due to secondary phase of $CaAl_2$ and $CaAl_4$ [38]. It is further noted that the foam containing 20 wt% SiCp exhibits primary peak aging at 6 h. In the case of 20 wt% SiCp composite foam, the microhardness values starts increasing after reaching a minimum at 8 h. These age-hardening curves thus demonstrate that aging in composite foam gets delayed with increases in SiCp content. It further states that 5 wt% and 10 wt%

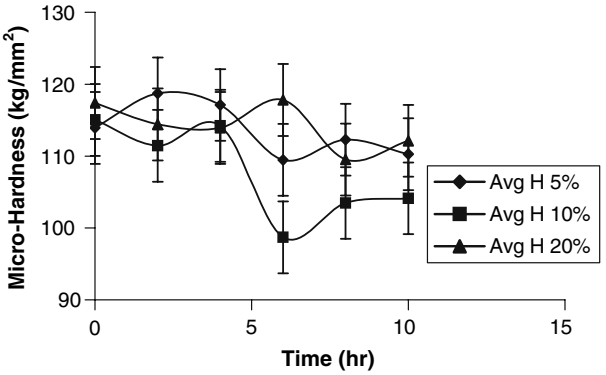

Fig. 6 Effect of aging time on the microhardness of aluminium foams containing different SiCp contents

SiCp composite foams aged faster than dense alloy. Out of these, the 10 wt% SiCp composite foam aged at the same time as that of composite. On the other hand, 20 wt% SiCp composite foam aged more slowly as compared to the fully dense composite, but aged at the same rate as that of the monolithic alloy. It was, in general, also noted that the composite foam exhibits secondary age hardening peaks unlike that observed in the alloy and composites. This is attributed to the precipitation of $CaAl_2$, $CaAl_4$ precipitates which comes from the dissolution of Ca from CaH_2 during foaming and forming an intermetallic phase with aluminium. Typical microstructures of composite foam in under aged, peak aged and over aged conditions are shown in Fig. 7a, b and c, respectively. The precipitate coarsed significantly during over ageing.

It was noted that peak aging time increases with increases in SiCp content (Fig. 8) in Al composite foam, unlike that in the fully dense composite. In case of the fully dense composite, the peak aging time is invariant to SiCp content, but faster then the alloy. This is attributed to the fact that the during foaming considerable micro-porosities are generated in the plateau and cell walls due to dissolution of hydrogen gas and its evolution during solidification (Fig. 9a). The evolution of gas also led to weak interface bonding, which acts as stress releasing sites and dislocation sinks (Fig. 9b). The discontinuous interface and the micro-porosities may act to retard the diffusion within the solids. The micro-porosity and weak interface area increase with increases in SiCp content. As a result, the age-hardening kinetics reduces with increases in SiCp content in composite foam. It may be noted that the 5 wt% SiCp composite foam ages faster than either the monolithic alloy or the fully dense composite. This is attributed to the fact that the effective cooling rate in case of composite foam is faster than that of solid alloy and composite because of significantly higher surface area of the cells exposed during

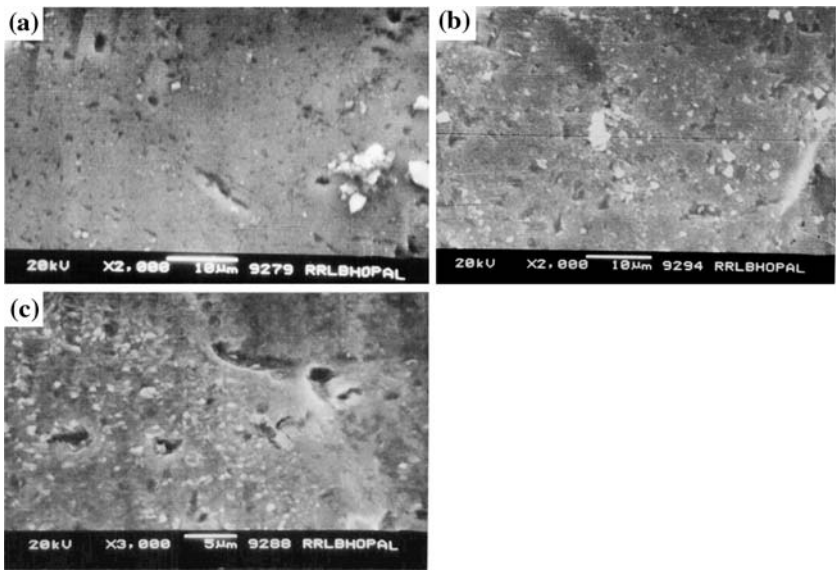

Fig. 7 Secondary electron images showing (**a**) limited precipitation in the matrix region of closed cell aluminium foam after aging for 2 h; (**b**) the extent of precipitation at the peak aging condition (6 h); (**c**) the coarsening of precipitates during over aging (8 h)

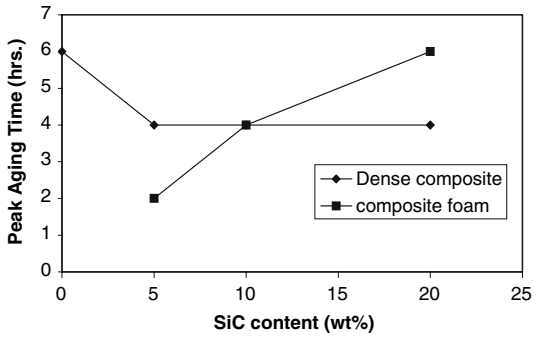

Fig. 8 Curve showing the relationship between the peak aging time and the percentage of SiCp content in aluminium foam and in a dense composite

quenching after solutionizing. The higher rate of quenching is expected to lead to higher degree of quenching stress and more dislocation density. The poisoning effect of microporosity and weak interface (interface incoherency) may be overpowered by the effect of significantly higher quench stress vis-à-vis higher dislocation density.

Conclusions

1. Addition of SiCp in fully dense composites accelerate aging behavior (precipitation and coarsening of precipitates) as compared to the monolithic alloy. The aging kinetics is invariant to SiCp content, however, above a threshold SiCp loading.
2. In the case of the composite foam, the aging kinetics is different when compared to the fully dense composite. The foam containing 5 wt% SiCp exhibits accelerated aging as compared to composite. When the SiCp increased to 10 wt%, the foam exhibits primary peak aging times similar to that of the fully dense composite. At further increases in SiCp to 20 wt%, however, the primary peak aging time of foam increased to 6 h, which is similar to that of monllithic alloy.

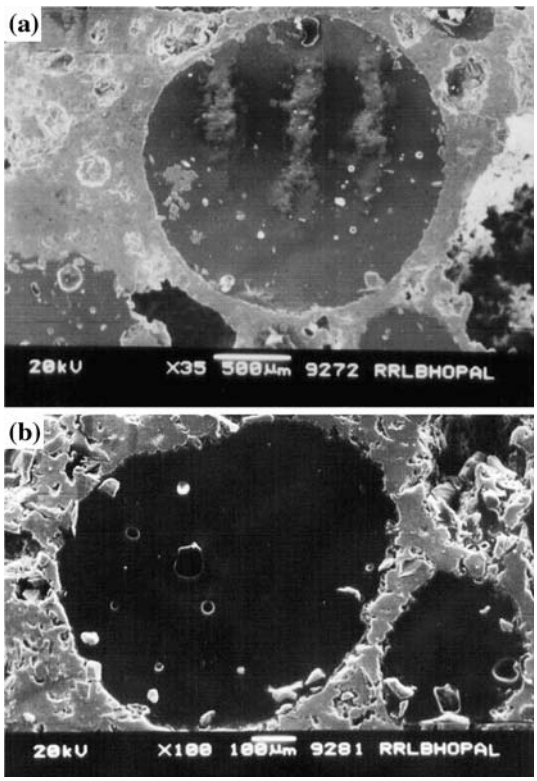

Fig. 9 Secondary electron images of the composite foam showing (**a**) microporosities in the cell wall and plateau region, and (**b**) weak interface between SiCp particles and matrix and large amount of SiCp particles in cell wall and plateau region

3. In foam, in addition to the primary aging, a secondary aging behavior due to precipitation of $CaAl_2$ and $CaAl_4$ is noted.
4. The peak aging time in composite foam increases with increases in SiCp content. This is attributed to increased porosity and, very weak SiCp matrix interface, which retard the nucleation as well as growth behavior of precipitates.

References

1. Smagorinski ME, Tsantrizos PG, Grenier S (1998) Mater Sci Eng A244:86
2. Frores FH (1994) Mater Sci Eng A184:119
3. Lloyd DJ (1994) Int Mater Rev 39:1
4. Kim BG, Dong SL, Park SD (2001) Mater Chem Phys 72:42
5. Gui M, Kang SB (2000) Mater Lett 46:296
6. Venkataraman B, Sundararajan G (2000) Wear 245(1–2):22
7. Iwai Y, Honda T, Miyajima T, Iwasaki Y, Surappa MK, Xu JF (2000) Compos Sci Technol 60:1781
8. Mondal DP, Das S, Rao RN, Singh M (2005) Mater Sci Eng A402:307
9. Watson G, Forster MF, Lee PD, Daswood RJ, Hamilton RW, Chirazi A (2005) Composites Part A 36:1177
10. Evans RD, Boyd JD (2003) Scripta Mater 49:59
11. Ferry M, Mounroe PR (2003) Mater Sci Eng A358:142
12. Calhoun RB, Dunand DC (2000) In: Kelley A, Zweben C (eds) Comprehensive Composite Materials. Vol. 3, Metal Matrix Composites (Vol. ed. Cline TW), Elsevier, pp.27–59
13. Mondal DP, Basu K, Narayan SP (2000) J Mater Sci Lett 19:1189
14. Dutta I, Bourell DL (1990) Acta Metall Mater 38:2041
15. Srivatson TS, Al-Hairi M, Smith C, Petrardi M (2003) Mater Sci Eng A346:91
16. Feng AH, Geng L, Zhang J, Yao CD (2003) Mater Chem Phys 82:618
17. Martin E, Forn A, Nogue R (2003) J Mater Proc Technol 143–144:1
18. Chan KC, Tong GQ (2001) Mater Lett 51:139
19. Wang GS, Geng L, Zheng ZZ, Wang DZ, Yao CK (2001) Mater Chem Phys 70:164
20. Han BQ, Chan KC, Tue TM, Lau WS (1997) J Mater Proc Technol 63:395
21. Yadav S, Chichili DR, Ramesh KT (1995) Acta Metall Mater 43:4453
22. Guden M, Hall IW (2000) Compos Struct 76:139
23. Chowla KK, Esmacili AH, Datya AK, Vasudevan AK (1991) Scripta Metall Mater 25:1359
24. Dutta I, Allen SM, Hafley JL (1991) Metall Trans 22A:2553
25. Chin JY, Harald HE, Joachim B (1998) Adv Mater Proc 11:45
26. Hall IW, Guden M, Yu CJ (2000) Scripta Mater 43:51
27. Tedesco JW, Ross CA, Kufnnen ST (1993) J Sound Vibr 165:376
28. Kathryn AD, James LJ (2000) Mater Sci Eng A293:157
29. Ashby MF, Evans AG, Fleck NA, Gibson LJ, Hutchinson JW, Wadley HNG (2000) Metal foams—a design guide. Buterworth-Heinemann, Boston
30. Ip SW, Wang Y, Toguri JM (1999) Can Met Quart 38(1):81
31. Tang F, Xiao Z, Tang J, Jiang L (1989) J Colloid Interface Sci 131:498
32. Deqing W, Ziyuan S (2003) Mater Sci Eng A361:45
33. Lehmhus D, Banhart J (2003) Mater Sci Eng A349:98
34. Banhart J, Baumeister J (1998) J Mater Sci 33:1431
35. Han F, Zhu Z, Gao J (1998) Metall Mater Trans 29A:2497
36. Simancik F, Jerz J, Kovacik J, Minar P (1997) Kovove Mater 35:265
37. Ledbetter HM, Austin MW (1987) Mater Sci Eng A89:61
38. Notin M, Gachon JC, Hertz J (1982) J Chem Thermodyn 14(5):425